


RESEARCH ARTICLE

Radiocarbon dating of samples connected to rock-cut features at Myrina Kastro (Lemnos Island, Greece) and calculation of the regional marine reservoir effect in the Late Bronze Age in the Aegean Sea

Yorgos Facorellis¹ , Christina Marangou^{2*}, Maria Ntinou³ and Rena Veropoulidou⁴

¹Department of Antiquities and Works of Art Conservation, School of Applied Arts and Culture, University of West Attica, Aghiou Spyridonos, 122 43 Egaleo, Athens, Greece, ²Independent Researcher, ³Department of Archaeology, Faculty of Philosophy, School of History and Archaeology, Aristotle University of Thessaloniki, 54124 Thessaloniki, Greece and ⁴Greek Ministry of Culture, Museum of Byzantine Culture, 2 Stratou avenue, 54640 Thessaloniki, Greece

Corresponding author: Yorgos Facorellis; Email: yfacorel@uniwa.gr

Received: 28 April 2022; **Revised:** 05 April 2024; **Accepted:** 08 April 2024

Keywords: AMS dating; Lemnos; marine reservoir effect; Myrina Kastro; rock-cut features

Abstract

The Kastro peninsula constitutes the extension towards the West of Myrina, the Lemnos capital, on the western coast of the island, in the North Aegean Sea. The ongoing research project on rock-cut features and rock-art of this complex site included a five-year (2002–2007) subsurface investigation, during which, among other mobile finds, charcoal and seashell samples were also collected, associated *in situ* to rock-cut features. Subsequently, in an attempt to bring about information on the dating of the rock-cut site, an investigation based on ¹⁴C has also been undertaken. Therefore, the purpose of the present paper is the AMS dating of the unearthened anthropogenic deposits and the calculation of the regional marine reservoir effect during the end of the Late Bronze Age. Our results show that the age of the deposits is spanning from the 13th century BC till the 6th century AD. Moreover, the ¹⁴C ages of two pairs of charcoal-seashell samples showed that the mean marine reservoir age R(t) in this region from the 13th to the 10th centuries BC is 175 ± 59 ¹⁴C yrs and the mean local sea surface reservoir deviation ΔR is found to be -288 ± 108 ¹⁴C yrs (within 1σ).

Introduction

The Kastro peninsula (38°52′29″N, 23°03′19″E) constitutes the extension towards the West of Myrina, the Lemnos capital, on the western coast of the island, in the North Aegean Sea. The hilly Kastro headland consists of volcanic rocks, mainly dacites (Anonymous 1993; Fornadel et al. 2012, 89; Pe-Piper et al. 2009, 41) and attends up to approximately 116 meters (*Admiralty Chart 1998*, nr. 1636) above present sea level (Figure 1). The headland took its name from the Byzantine, Venetian, Genovese and Ottoman castle (“Kastro”) on its northern, highest part. The castle structures, edifices and triple enclosure were built and periodically restored from the 12c. AD onwards (Hellenic Ministry of Culture 1999, 56–57). Before Medieval and post-Medieval occupation, the rocks had been carved in several areas, creating anthropogenic structures, engravings and complexes within the natural landscape and seascape (Marangou 2009; 2020b; 2021) (Figure 2a). Due to polychromatic and morphological particularities, as well as to erosion and ulterior damage, it may be arduous to distinguish anthropogenic alterations from the natural rock. If rock-cut features and rock art are omnipresent on the whole

*Archaeologist, responsible for the research on Myrina Kastro rock-cut features and rock art, Athens, Greece



Figure 1. General view of the Myrina Kastro peninsula from the East. The ellipse shows the location of the sampling site. (photograph C. Marangou).

peninsula, including inside the castle walls and on the outskirts of the town, they are better preserved in areas that were less densely re-occupied. In all attested periods, the maritime connections of the Kastro rock-cut features and rock art are obvious, suggested not only by its close associations to the coast and the sea, but also by residues of seashells and materials arrived by sea, as well as by nautical representations (Marangou 2006, 2020b, 2021) (Figure 2b).

The ongoing research on rock-cut features and rock-art on Myrina Kastro is realized with the permission of the Greek Archaeological Service, the Local Council for the Monuments of the Islands and the Greek Ministry of Culture. In addition to the study of rock-cut structures and rock-art on the surface, the research project at Kastro included, during the years 2002–2007, a sub-surface investigation related to a number of selected rock-cut features, which permitted the collection of mobile finds, including organic materials, such as charcoal and seashells¹. The samples examined in this paper were found in the exterior of the castle fortification walls, in southern and eastern Kastro areas. The charcoal samples were found in four sectors of the peninsula, two of which provided the largest part, while two sea-shells were connected to charcoal samples in one of the latter sectors.

The present paper has two objectives, the first one is the radiocarbon dating with AMS of the investigated deposits, obviously associated to the aforementioned rock-cut features, and the second one the calculation of the regional marine reservoir effect in the Late Bronze Age in the Aegean Sea. The latter is part of a large-scale project, which is currently underway, to model the global sea-level rise within the Aegean Sea since the Last Glacial Maximum. The results of this project, when it will be completed, may shed light on the complex interaction between sea-level rise, ocean currents and the mixing of Mediterranean, Aegean and Black Seas' waters. This is done by calculating the marine reservoir effect $R(t)$, as well as the regional sea surface reservoir deviation ΔR from the global ocean model (Stuiver and Braziunas 1993), in various regions of the Aegean Sea, as it was found that this fluctuates considerably through time (Facorellis and Vardala-Theodorou 2015). The calculation of ΔR in every region is very important, as it allows the: (1) reliable calibration of the conventional ^{14}C ages of marine samples (e.g. marine mollusk shells), in the absence of other suitable material from an excavated

¹ The coauthors of this paper and other specialists are contributing to their publication in a volume in preparation.



Figure 2. (a) Rock-cut features of Kastro: flights of steps, channel, cavity, remains of vertical “panels/walls”. (b) Rock-art on Kastro: the rock-engraving of a rowed ship, probably dating from the Bronze Age, on the vertical surface of a rock-cut, stepped feature in the Myrina port (photographs C. Marangou).

site (as they are usually short-lived samples, rarely transported over long distances), (2) reliable calibration of ^{14}C ages of human bones in case of mixed (marine and terrestrial) diet (Sveinbjörnsdóttir et al. 2010), and (3) obtaining of paleoceanographic information (Siani et al. 2001). The Kastro research offered the opportunity to provide suitable material for such a parallel study and its results are presented together with the archaeological ones.

Materials

During a five-year period (2002–2007) of subsurface investigation campaigns, among other mobile finds, numerous charcoal and seashell samples were collected. The ellipse in Figure 1 shows the location of the sampling site on the Myrina Kastro hill. In this study, the AMS dates of 19 samples (17 charcoal pieces and 2 seashells) are presented.

All charcoal pieces were taken from carbonized wood. Their species have been identified by an anthracological study of the carbonized material unearthed (Table 1). The charcoal samples Lyon-17628(GrM) and Lyon-17627(GrM) were identified as *Angiosperms*. The taxon *Angiosperm* includes

Table 1. Summary of the AMS radiocarbon dating results of the samples from the Myrina Kastro (subsurface research 2002–2007), Lemnos sorted by increasing age. (msl = mean sea level). (Numbered strata refer to investigated horizontally or/and vertically distinct deposit units)

Lab code nr.	Sample location	Type of sample – species	Date of collection	$\delta^{13}\text{C}$ (‰)	^{14}C age (yrs BP)	Calibrated age (yrs)	Probability (%)
Lyon-17629(GrM)	Sample Nr. 10, Sample from pottery nr. 8, Area NA/A1a, Stratum 1, from channel inside carved rock, 29 m from msl	Charcoal – <i>Olea europaea</i>	08-07-04	–24.6**	1675 ± 60*	255–528 AD 248–539 AD	68.3 95.4
Lyon-19724(GrM)	Sample Nr. 14, Sample 4 from NK 9, Area N/Z, W area, 1.12 m N × 2.55 m W, Stratum 6, 39 m from msl	Charcoal – <i>Quercus sp. deciduous</i>	24-10-02	–27.3**	1990 ± 60*	46 BC–117 AD 150 BC–205 AD	68.3 95.4
Lyon-16562(GrM)	Sample Nr. 7, Find sample nr. 3, Area N/Z, Stratum upper part of 6, western area, 2.54 m N × 0.87 m W, 39 m from msl	Charcoal – <i>Olea europaea</i>	24-10-02	–25.2**	2020 ± 60*	98 BC–78 AD 196 BC–155 AD	68.3 95.4
Lyon-16561(GrM)	Sample Nr. 5, Find sample nr. 30, Area N/Z, Stratum 6, 0.88 m S × 3.60 m W, 39 m from msl	Charcoal – <i>Quercus sp. deciduous</i>	01-07-03	–26.0**	2020 ± 60*	98 BC–78 AD 196 BC–155 AD	68.3 95.4
Lyon-19722(GrM)	Sample Nr. 8, Find Sample Nr. 31, Area N/Z, Stratum 6, 1.0 m N × 4.0 m W, 39 m from msl	Charcoal – <i>Quercus sp.</i>	1-07-03	–24.7**	2020 ± 60*	98 BC–78 AD 196 BC–155 AD	68.3 95.4
Lyon-16563(GrM)	Sample Nr. 9, Soil sample nr. 31, Area N/Z, Stratum 5, 0.73 m N × 3.47 m W, 39 m from msl	Charcoal – <i>Quercus sp. deciduous</i>	01-07-03	–24.9**	2030 ± 60*	102 BC–66 AD 197 BC–126 AD	68.3 95.4
Lyon-16564(GrM)	Sample Nr. 12, Find sample nr. 2 from NK 6, Area N/Z, Stratum 4-5, western area, 1.36 m N × 3.27 m W, 29 m from msl	Charcoal – <i>Olea europaea</i>	23-10-02	–24.0**	2040 ± 60*	148 BC–59 BC 197 BC–121 AD	68.3 95.4
Lyon-19721(GrM)	Sample 6, Area N/Z, Stratum 5, NW area, 3.38 m N × 0.25 m W, 39 m from msl	Charcoal – <i>Quercus sp. evergreen</i>	21/10/02	–26.1**	2050 ± 60*	153 BC–23 AD 341 BC–118 AD	68.3 95.4
Lyon-19723(GrM)	Sample Nr. 11, Find sample Nr. 30, Area N/Z, 0.88 m S × 3.60 m W, over the rock, 39 m from msl	Charcoal – <i>Quercus sp. deciduous</i>	1-07-03	–24.5**	2100 ± 60*	198–42 BC 356 BC–58 AD	68.3 95.4
Lyon-17630(GrM)	Sample Nr. 13, Sample nr. 3 from soil sample nr. 7, Area N/Z, Stratum (4)-5, on the rock, west of “N wall”, 1.02 m N × 3.59 m W, 29 m from msl	Charcoal – <i>Fabaceae</i>	23-10-02	–25.3**	2105 ± 30	165–55 BC 337–43 BC	68.3 95.4
Lyon-16566(GrM)	Sample Nr. 16, Find sample nr. 5, Area N/Z, Stratum 6, western area, from carved cavity, 0.68 m N × 3.21 m W, 39 m from msl	Charcoal – <i>Pistacia lentiscus</i>	24-10-02	–22.7**	2120 ± 30	176–56 BC 342–49 BC	68.3 95.4

Lyon-17628(GrM)	Sample Nr. 3, Find sample nr. 34, Area N/Z, Stratum 6, NW angle, 1.26 m S × 3.10 m W, 29 m from msl	Charcoal – <i>Angiosperm</i>	04-07-03	–29.9**	2195 ± 30	356–196 BC 366–171 BC	68.3 95.4
Lyon-17627(GrM)	Sample Nr. 1, from soil sample nr. 1ep, Area N/E 3.3, Stratum 3, among pottery sherds, from W-E channel, 0.48 m S × 2.65 m W, 29 m from msl	Charcoal – <i>Angiosperm</i>	07-07-04	–24.1**	2205 ± 30	358–200 BC 371–176 BC	68.3 95.4
Lyon-16567(GrM)	Sample Nr. 17, Soil sample nr. NK 1, Area NA/A5a, Stratum under the layer with stones, 29 m from msl	Charcoal – <i>Olea europaea</i>	10-07-06	–22.9**	2825 ± 60*	1105–902 BC 1192–830 BC	68.3 95.4
Lyon-16559(GrM)	Sample Nr. 2, sample 1, upper part of soil sample nr. 3ep, Area NA/A5a, Stratum 8, SW angle, 29 m from msl	Charcoal – <i>Phillyrea/Rhamnus</i>	14-07-04	–26.4**	2860 ± 30	1107–941 BC 1122–927 BC	68.3 95.4
Lyon-16560(GrM)	Sample Nr. 4, Soil sample nr. 2, Area NA/A5a, Stratum 8, SW angle, 29 m from msl	Charcoal – <i>Erica sp.</i>	14-07-04	–26.2**	2875 ± 30	1112–1008 BC 1192–931 BC	68.3 95.4
Lyon-16569(GrM)	Shell 2, Soil sample nr. 2ep, Area NA/A5a, Stratum 8, SW angle, 29 m from msl	Seashell – <i>Patella caerulea</i> L.,1758	14-07-04	–2.0***	3055 ± 30	1217–906 BC 1369–786 BC	68.3 95.4
Lyon-16565(GrM)	Sample Nr. 15, soil sample nr. 3ep, Area NA/A5a, Stratum 8, SW angle, 29 m from msl	Charcoal – <i>Phillyrea/Rhamnus</i>	14-07-04	–24.4**	2965 ± 30	1225–1124 BC 1271–1055 BC	68.3 95.4
Lyon-16568(GrM)	Shell 1, Soil sample nr. 3ep, Area NA/A5a, Stratum 8, SW angle, 29 m from msl	Seashell – <i>Patella caerulea</i> L.,1758	14-07-04	–0.9***	3135 ± 30	1324–1005 BC 1457–861 BC	68.3 95.4

**“Old wood” corrected ¹⁴C ages with the subtraction of 100 ± 50 yrs from the measured ones (see text).

**AMS measured value.

***IRMS measured value.

charred wood remains that present anatomy features of the xylem of the flowering plants, but in the case of the aforementioned samples, their identification to family, genus or species level was not feasible due to bad preservation. The ^{14}C ages obtained for the species *Quercus sp. deciduous* and *Olea europaea* can be older due the “old wood effect”. In order to compensate for this potential effect, an approximate correction to the charcoal dates of the aforementioned long-lived species was applied by subtracting 100 ± 50 ^{14}C yrs from the ^{14}C ages. For instance, ± 50 yrs were added in quadrature to the measured uncertainty of ± 30 yrs of their ^{14}C ages. Therefore, for the ^{14}C ages of the samples Lyon-17629(GrM), Lyon-19724(GrM), Lyon-16562(GrM), Lyon-16561(GrM), Lyon-19722(GrM), Lyon-16563(GrM), Lyon-16564(GrM), Lyon-19721(GrM), Lyon-19723(GrM) and Lyon-16567(GrM), an increased uncertainty of ± 58.3 yrs (rounded to 60 yrs) was used for their calibration (Table 1).

The charcoal/seashell pairs of samples [Lyon-16565(GrM)/Lyon-16568(GrM) and Lyon-16560(GrM)/Lyon-16569(GrM)] were named Myrina-1 and Myrina-2 (Table 2), respectively. Both samples of each pair were collected exactly in the same location and depth (Table 1) from undisturbed anthropogenic deposits, thus ensuring that all pairs of samples were deposited simultaneously in the past. However, these two pairs were found in slightly different locations and depths at the SW angle and stratum 8 of the area NA/A5a.

The charcoal sample of the Myrina-1 pair belong to the short-lived tree species *Phillyrea/Rhamnus*, whereas the one of Myrina-2 pair belong to the short-lived tree species *Erica sp.*

The seashells of both pairs belong to the species *Patella caerulea* L., 1758, which is a short-living grazing gastropod species that inhabits the midlittoral and upper intralittoral coastal zones. They have a limited spatial mobility, thus after moving around to graze, they return to their original habitat zone. Though they withstand exposure to wave action, they mainly colonize sheltered areas (Banister 1975; Davies 1969; Seila 1993).

Methods

All samples were chemically pretreated in the Centre de Datation par le RadioCarbone in Lyon, France, and graphitized (Aerts-Bijma 1997) and measured in the radiocarbon dating facility of the Centre for Isotope Research (CIO) in Groningen, Netherlands (van der Plicht 2000; Wijma 1997).

The usual acid-base-acid (ABA) protocol was applied for the chemical pretreatment of the charcoal samples. According to this protocol, the samples are roughly crushed before being treated with 2N HCl (room temperature, 1 hr then 4 hr at 95°C), followed by 0.1N NaOH (room temperature, 1 hr then 1 hr at 95°C), and then treated with 2N HCl (room temperature, 1 hr). The samples are washed 3 times with ultrapure MilliQ™ deionized water after each treatment.

After pretreatment, the charcoal samples are combusted in an automated Thermo Finnigan Flash EA 1112 (EA). The EA consists of a Cr_2O_3 combustion tube, a cobaltous/ic oxide silvered purification furnace, a Cu reduction tube, and a water trap. The EA system is expended with an automatic cryogenic trapping device. This system consists of 16 separate freeze fingers in a vacuum system. Each trap has a pneumatic valve and a Dewar vessel filled with liquid nitrogen. The CO_2 of each sample is collected cryogenically in a glass ampoule and sealed.

The treatment of the seashell samples involved a surface cleaning by air abrasion with aluminium oxide powder to remove the outer surface and rinsing with ultrapure water. Then the seashells were etched with aqua regia (0.5–1.0N HCl and HNO_3 , 3:1) until 10–30% of the sample has been removed to eliminate the surface contaminants (Goslar and Pazdur 1985). The samples were then dried and roughly crushed (Hedges 1989). Afterwards, the samples were reacted with H_3PO_4 (3 mL, 85%) under vacuum in a two-armed Pyrex reaction vessel. The reaction vessels were transferred to a water bath at 60°C and left to equilibrate for an hour to ensure a complete reaction to avoid fractionation effects, before adding the acid to the samples and leaving to react overnight. The CO_2 obtained from each sample was transferred to a glass ampoule and sealed (Facorellis et al. 2017).

Table 2. Regional marine reservoir effect $R(t)$ and local deviation ΔR values for Myrina-1a, Myrina-1b and Myrina-2 charcoal/seashell pairs from the Myrina Kastro, Lemnos

Pair	Labe code nr.	Type of sample – species	^{14}C age (yrs BP)	$R(t)$ (^{14}C yrs)	ΔR (^{14}C yrs)	Probability (%)
Myrina-1	Lyon-16565(GrM)	Charcoal – <i>Phillyrea/Rhamnus</i>	2965 ± 30	170 ± 42	–294 ± 77	68.3
	Lyon-16568(GrM)	Seashell – <i>Patella caerulea</i> L.,1758	3135 ± 30		–296 ± 153	95.4
Myrina-2	Lyon-16560(GrM)	Charcoal – <i>Erica sp.</i>	2875 ± 30	180 ± 42	–282 ± 76	68.3
	Lyon-16569(GrM)	Seashell – <i>Patella caerulea</i> L.,1758	3055 ± 30		–281 ± 152	95.4
Mean values				175 ± 59	–288 ± 108	68.3
					–289 ± 216	95.4

The stable isotopic values ($\delta^{13}\text{C}$) of the seashell samples were measured on an isotope ratio mass spectrometer (IRMS) at the Institut des Sciences Analytiques (ISA) in Lyon, France, whereas those of the charcoal samples were measured by AMS in CIO (Table 1).

Results and Discussion

I. Calculation of the Regional Marine Reservoir Effect

The regional marine reservoir effect $R(t)$ value of each pair is calculated by subtracting the ^{14}C conventional age of the charcoal sample from that of the marine mollusk sample (Facorellis and Vardala-Theodorou 2015; Siani et al. 2000, 2001; Stuiver et al. 1986, 1998; Stuiver and Braziunas 1993). These are $R(t) = 170 \pm 42$ ^{14}C yrs for Myrina-1 pair [samples Lyon-16565(GrM) and Lyon-16568(GrM)] and 180 ± 42 ^{14}C yrs for Myrina-2 pair [samples Lyon-16560(GrM) and Lyon-16569(GrM)]. The $R(t)$ values of both pairs overlap within 1σ . This consistency thus enables the calculation of a mean $R(t)$ value of 175 ± 59 ^{14}C yrs (Table 2). The $R(t)$ and mean $R(t)$ uncertainties were calculated using the following general formula for summing uncertainties:

$$\sigma_x = \sqrt{\sigma_1^2 + \sigma_2^2} \quad (1)$$

where x represents $R(t)$ or mean $R(t)$, and σ_1 and σ_2 are the uncertainties associated with the summed values.

The estimated regional mean $R(t)$ age for the late Bronze Age (from the 13th to the 10th centuries BC) in the Aegean Sea appears to be considerably lower than the modern pre-bomb $R(t)$ age 520 ± 40 ^{14}C yrs reported by Siani et al. (2000), which was found to be the same with the $R(t)$ age 515 ± 22 ^{14}C yrs for the end of the 8th millennium to the beginning of the 7th millennium BC reported by Facorellis et al. (1998). However, it has been shown that the $R(t)$ ages in the Aegean Sea fluctuate with time (Facorellis and Vardala-Theodorou 2015). Lemnos features a diverse terrain characterized by sedimentary and volcanic rocks. The western part of Limnos, where Myrina Kastro lies, showcases a rugged topography, while the eastern portion is characterized by lower elevations and a smoother landscape (Gläser et al. 2022). However, the Kastro hill consists of volcanic rocks, and its surrounding area between Roméikos Yalos (Greek Coast) and the old port of Myrina consists of sandstone. Additionally, a little further north at Avlona beach, as well as a little further south at Plati bay, there are alluvial and colluvial deposits indicating the action of freshwater (Panagopoulos et al. 2013; Pavlopoulos et al. 2013). Nevertheless, the much lower and consistent, within almost 100 years, $R(t)$ ages of both Myrina pairs cannot be attributed to freshwater effects. If this were the case, they would have been much higher due to the incorporation of geological age carbon in the sea mollusk shells. On the contrary, this may be due to a more rapid circulation of the sea surface water. This is probably caused by different sea surface temperatures or sapropel formation conditions (Mercone et al. 2000; Casford et al. 2002) in the Aegean Sea in the late Bronze Age than those prevailing during the aforementioned time periods.

The ΔR values were calculated with the OxCal v4.4.4 software (Bronk Ramsey 2009) employing a Bayesian probability method (Facorellis and Vardala-Theodorou 2015). The routines for these calculations can be found in an appendix in the online version of this paper. For both pairs of samples, the uniform likelihood function $U(x_1, x_2)$ was set, with $x_1 = -550$ and $x_2 = 100$, to impose constraints on the potential range of ΔR (Bronk Ramsey and Lee 2013). Figure 3 shows the probability distribution plots for (a) the Myrina-1 [Lyon-16565(GrM)—Lyon-16568(GrM)] pair, $\Delta R = -294 \pm 77$ ^{14}C yrs (within 1σ) and (b) the Myrina-2 [Lyon-16560(GrM)—Lyon-16569(GrM)] pair, $\Delta R = -282 \pm 76$ ^{14}C yrs (within 1σ) (Oxcal v.4.4.4 Bronk Ramsey 2009). Since these values overlap within 1σ , the local mean sea surface reservoir deviation ΔR value calculated from both pairs² is -288 ± 108

² The mean ΔR uncertainty was also calculated using the general formula (1).

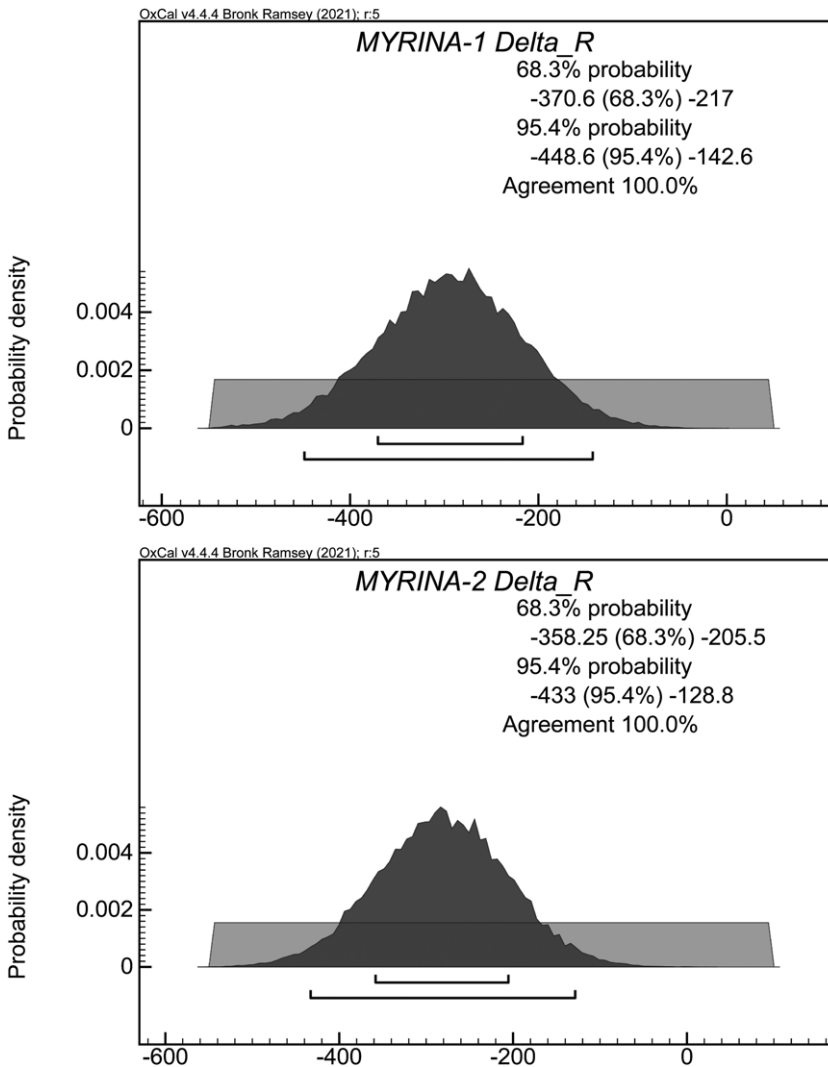


Figure 3. Probability distribution plots for (a) the Myrina-1 [Lyon-16565(GrM)—Lyon-16568(GrM)] pair, $\Delta R = -294 \pm 77$ ^{14}C yrs (within 1σ) and (b) the Myrina-2 [Lyon-16560(GrM)—Lyon-16569(GrM)] pair, $\Delta R = -282 \pm 76$ ^{14}C yrs (within 1σ) (Oxcal v.4.4.4 Bronk Ramsey 2009).

^{14}C yrs (Table 2). It is worth noticing that it is the first time that $R(t)$ and ΔR are calculated for the late Bronze Age, thus adding a piece of information on the model of the global sea-level rise within the Aegean Sea.

The conventional ^{14}C ages of the charcoal samples were calibrated with the latest issue IntCal20 of the atmospheric international calibration curve (Reimer et al. 2020). The ^{14}C ages of the seashell samples were calibrated using the aforementioned mean ΔR value (within 1σ) in conjunction with the latest issue Marine20 of the international marine calibration curve (Heaton et al. 2020). All calibrations were also performed with the OxCal v4.4.4 software. Table 1 presents the samples laboratory code, location, species, the obtained ^{14}C and calibrated ages and the corresponding $\delta^{13}\text{C}$ values sorted by increasing age. The calibrated ages are given using the minimum and maximum for all the probability distribution intervals within 68.3 and 95.4%. At the same time, archaeological data of contexts related to the samples seem to suggest the Late Bronze Age for sector II.1 (NA/A5a), mainly the Hellenistic period, around 300 BC or 3rd century BC for sectors II.2a and II.2b (N/Z and N/E), and Late Antiquity,

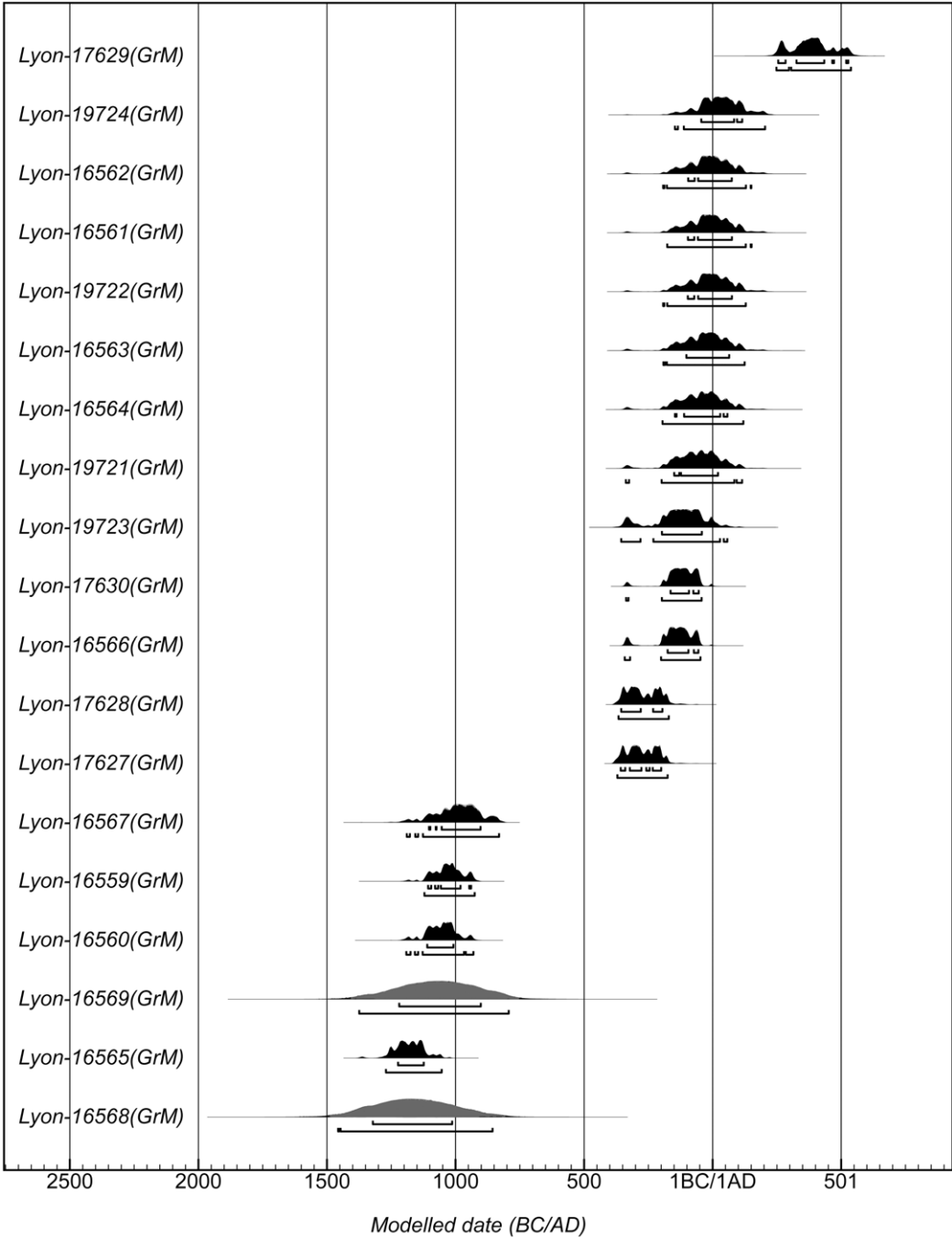


Figure 4. Probability distribution plots of the calibrated dates from the Myrina Kastro (subsurface research 2002–2007) sorted by increasing age. Black color and gray colors indicate calibrated dates obtained from charcoal and seashell samples using the IntCal20 and Marine20 international calibration curves, respectively (Oxcal v.4.4.4 Bronk Ramsey 2009).

possibly 4th century AD for sector II.3 (NA/A1a) (see further). However, a table containing all the probability distribution intervals of each calibrated age can also be found online in the appendix. Figure 4 shows the probability distribution plot of the calibrated dates from the Myrina Kastro sorted by

increasing age. Black and gray colors indicate calibrated dates obtained from charcoal and seashell samples using the IntCal20 and Marine20 international calibration curves, respectively (Oxcal v.4.4.4 Bronk Ramsey 2009).

II. Rock-Cut Features Connected to the Dated Samples

The samples are all associated to rock-cut features on Myrina Kastro. The current results of the radiocarbon dating seem to confirm that the investigated areas providing the samples were not significantly disturbed by posterior occupation in Medieval and later times, while mobile finds with contextual relations to the analyzed samples are apparently consistent with their ^{14}C dating. According to the current state of research, a part of the mobile finds being still under study, our results show that the investigated subsurface anthropogenic deposits related to selected rock-cut features of the site date from the 13th century BC until the 6th century AD.

II.1 13th–10th centuries BC (Late Bronze Age–Early Iron Age)

On a road side, in front of a stepped dead end

[charcoal samples Lyon-16560(GrM), Lyon-16565(GrM), Lyon-16559(GrM), Lyon-16567(GrM), and seashells Lyon-16568(GrM) and Lyon-16569(GrM)]

The earliest dated charcoal samples were collected in a restricted area of up to three square meters. They were found in limited spaces in immediate proximity to or under three vertically set stones forming a rough triangle, the latter located in front of a carved flight of narrow steps ending into the rock without any further issue (Marangou 2020a). Such dead ends, stairs leading nowhere and/or ending to niches, some of them called “stepped altars”, have numerous Bronze Age–Iron Age parallels in Thrace and Anatolia in particular, but also in the Aegean (see references in Marangou 2009, 2020a, 2020b). This restricted space is situated, at the same time, at crossroads, on the side of a rocky passageway, the latter intersected by three different flights of steps; thus both physical and symbolic itineraries would be combined here (Marangou 2020a; 2021). The context of the samples included mainly Late Bronze Age (possibly at least 13th–12th century BC) mobile finds, their dating consistent with that of the samples. Besides fragments of pottery and clay objects, a lot of animal bones and seashells were also found in this area³, while fragments of figurines and tools mostly related to female activities come from strata slightly later than those of the samples.

A charcoal sample Lyon-16560(GrM) shows a date of 1112–1008 cal BC⁴. A further charcoal sample Lyon-16565(GrM) coming from a lower level, dates to the Late Bronze Age: 1225–1124 cal BC. The charcoal sample Lyon-16559(GrM): 1107–941 cal BC was found slightly over the sample Lyon-16565(GrM). The context of the sample Lyon-16567(GrM): 1105–902 cal BC, which was not found in connection to the dated shells, comprised organic residues, including a few grains. This sample was related to a group of flat stones horizontally placed, partly located under the vertically set stones, although not necessarily *stricto sensu* connected to the latter. At the lowest limit of the investigation in this particular spot, it would be slightly later or even contemporaneous to the neighbouring earliest sample (Lyon-16565(GrM)).

II.2 4th century BC–1st century AD (mainly Hellenistic, possibly also Late Classical periods)

Most samples but one furnishing dates from approximately the 4th century BC to the 1st century AD come from one of two sectors. As both sectors are rather extended, it is the spaces having furnished the samples that can be dated to these periods, while other zones of one of the areas in particular may also indicate earlier occupation.

³ Preliminary presentations of this ensemble: Marangou et al. (2014); Marangou (2020a).

⁴ All calibrated dates in text are given within 1σ .

II.2.a Carved conduits and cavities, rock-cut “walls” and an open sea-view. [charcoal samples Lyon-19724(GrM), Lyon-17630(GrM), Lyon-16562(GrM), Lyon-16561(GrM), Lyon-16566(GrM), Lyon-19722(GrM), Lyon-16563(GrM), Lyon-16564(GrM), Lyon-19721(GrM), Lyon-17628(GrM) and Lyon-19723(GrM)]

A large sector with several charcoal samples repeatedly indicates dates spanning from the 4th century BC until the 2nd century AD (356 cal BC–117 cal AD). This extended sector includes carved cavities and conduits, including a large channel, on a rock floor, probably for the management of liquids (Marangou 2006, 2009) and remains of stone wall foundations, as well as a rock “wall” with openings orientated towards the sea and associated to a rock-cut platform with “seats” (Marangou 2006; alleged aniconic “thrones” for divinities: Marangou 2020b with references). These conspicuous rocks could also have constituted a seamark for mariners, offering at the same time a wide-ranging view of the harbour and approaching ships (Marangou 2016; 2020b). Most samples were found in a zone comprising carved conduits and cavities. Comparatively earlier samples were found in a restricted zone, almost immediately over the rock surface. The sector provided various finds (possibly dating from around 300 BC, or the 3rd century BC at the latest). Among others, fragments of pottery and clay objects, such as lamps and tools related to female everyday tasks and female figurines (Marangou 2009, 2016), as well as metal artefacts, including coins and possible residues of metal elaboration⁵ (Marangou 2006), were also found. Taking account of the location of this area as a convenient observation post and according to evidence about maritime trade and possibly metal elaboration, practical uses are combined here with ritual functions (Marangou 2009, 2016, 2020b, 2021).

II.2.b Open-air ritual spaces, stepped ramps and a passageway overlooking the coast. [charcoal sample Lyon-17627(GrM)]

An isolated sample Lyon-17627(GrM) provides similar dating (358–200 cal BC) and was found in a sector comprising a carved passageway with an East-West orientation, at the edge of the rocks overlooking the coast, more or less parallel to it⁶. The sample was found among pottery sherds, in one of the East-West channels of the zone.

This sector shows a long continuity of use, concrete, but also symbolic, as it includes probable open-air ritual spaces, apparently of different periods. If stepped rocks and carved panels on the road side possibly date to the Bronze or Iron Age (Marangou 2020a), figurines and clay artefacts (Marangou 2006, 2009), were possibly related to an open air, small stone “altar” (Late Classical?) in a zone of this sector (Marangou 2020b) and various finds, such as pottery (under study), on the major part of the main passageway, its channels and structures, would date mainly from the Late Classical to the Hellenistic (the latter approximately 3rd century BC) periods. Descending flights of steps crossing the thoroughfare are directed towards the coast, with more ramps or trails leading lower to the seaboard, while the area offers again an open view to the sea (Marangou 2006, 2020a, 2021). Furthermore, “special” spaces at crossroads between a road and flights of steps would suggest again a symbolic—combined with the practical—function of itineraries in this transitional, therefore liminal area (Marangou 2021), considering in particular the passage from the coastal area and the sea to the Kastro flanks and *vice versa* (Marangou 2020a, 2020b). Cult of female divinities of nature and/or liminality, such as the goddesses Lemnos, Cybele and Artemis, are indeed attested on the island since at least the Archaic period⁷, and present similar iconographic characteristics (*polos* headgear, “throne”) with the Kastro figurines (Marangou 2016), while at least one rock-cut “Cybele façade” was identified elsewhere on Kastro (Marangou 2021).

⁵ Results of residue analyses under study.

⁶ The results of analyses of possible residues of metal elaboration in this sector are currently under study.

⁷ On figurines and cult of female goddesses in Myrina and surrounding areas see, among others: Archontidou-Argyri (2000); Beschi (2001); Filaniotou (2012); on Lesbos figurines see Acheillara (2005); on the cult of Cybele in the northeast Aegean see Rouggou (2013).

II.3 3rd–4th centuries AD (Late antiquity)

A rock-cut “chamber” with niches, channels and cavities, under a rock formation

[charcoal sample Lyon-17629(GrM)]

Finally, the latest of our samples Lyon-17629(GrM) was found in a carved channel around a shallow rounded cavity on a partly preserved rock floor with a pit. The channel is situated to the left of a rock-cut vertical “wall/panel” with angled, narrow extensions on both sides and a platform in front, under a partly carved formation, the latter including a few niches with linear carvings and rock-cut steps (Marangou 2009; 2020b). The channel also contained pottery sherds, as well as a metal artefact and an iron(?) fragment. The calibrated date of the sample is 255–528 cal AD. Late antique visiting or re-use, possibly in the 4th centuries AD according to mobile finds, of earlier (possibly Iron Age) rock-cut features, such as a stepped rock and carved cavities and conduits, possibly with additional rock modifications, seem possible.

Conclusions

Studied for the first time in Lemnos, the Kastro rock-cut features cover most sectors of the peninsula on various altitudes and present complex patterns of typology, location, setting, function and chronology (Marangou 2012, 2020b). The current state of research suggests some interpretative directions concerning preferences for types of structures, intercommunication, connections between zones and hypotheses for symbolic and/or concrete functionalities (Marangou 2019). If relative dating of rock-cut features may be possible based on evidence of contextually connected mobile finds when available, radiocarbon dating obviously proves crucial. Our results till now confirmed the time span of use of some types of rock-cut features, but also pointed out either their contemporaneity, or their resilience and diachronic use in some cases.

The earliest dated samples (13th–10th centuries BC) would be related to the Late Bronze Age part (possibly at least 13th–12th century BC) of a probable symbolic Late Bronze Age–Early Iron Age deposit in connection to a three stones arrangement and a so-called “stepped altar”, located at crossroads, to the side of a passageway, the latter also implying accessibility to the spot, while access to the upper part/end of the narrow steps would rather be restricted. Despite the fact that this space is invisible from the sea, it presents obvious maritime links: seashells, but also ship graffiti on sherds (Marangou 2020b).

In the periods from the 4th century BC to the 2nd century AD (mainly Hellenistic, 3rd century BC or around 300 BC, and possibly also Late Classical), the contextual information of our samples indicates associations to probable open-air ritual spaces with both visual and material links towards the coast, the sea and the seascape. One sample was found in a road zone, in which some “significant” places of different periods were apparently located, while the majority of the samples were found in a large area with several carved features, both into the rock floor and on structured complexes, which furnished important mobile finds. A parallelism of concrete and symbolic functions seems possible: the practical accessibility of “special” *loci* via a passageway and stepped ramps and the possible additional use of symbolic spaces as observation posts may be combined in these periods with evidence suggesting trade and industrial activities. In the Kastro complex volcanic seascape (Marangou 2019, 2021), the sea constitutes a most determining factor, as well as a particularity in comparison to other rock-cut sites.

The late antiquity (3rd–6th centuries AD) sample was found in a channel around a cavity, associated to a rock-cut “chamber” in front of a rock with carved steps and niches. A later visit or re-use, possibly in the 4th century AD, of earlier rock features seems possible in this case. Here, as well as in the above-mentioned area, comprising open-air particular spaces of different periods, a diachronic use is conceivable, even if precise space attribution and/or function were modified. This evidence could indicate symbolically and/or materially significant zones occupied through late prehistory and antiquity, and therefore offers evidence for the permanency of meaningful places (Marangou 2020a).

In addition, the radiocarbon dating of two charcoal/seashell pairs of samples allowed the calculation for the first time of the regional marine reservoir effect $R(t)$ and the local sea surface reservoir deviation ΔR in the late Bronze Age in the Aegean Sea. The mean $R(t)$ value in this region from the 13th to the 10th centuries BC is 175 ± 59 ^{14}C yrs and the local mean sea surface reservoir deviation ΔR is found to be -288 ± 108 ^{14}C yrs.

Supplementary material. To view supplementary material for this article, please visit <https://doi.org/10.1017/RDC.2024.69>

Acknowledgments. Christina Marangou is most grateful to the Ephorate of Antiquities of Lesvos (formerly K' Ephorate of Prehistoric and Classical Antiquities), the Local Council for the Monuments of the Islands and the Greek Ministry of Culture for granting permission for the on-going research project and publication of the rock-cut features and rock-art, including subsurface investigation (2002–2007) and its mobile finds, at Myrina Kastro. Special thanks are due to Dr Pavlos Triantafyllidis, director of the Ephorate of Antiquities of Lesvos, for kindly permitting to conduct analyses of material from the subsurface research and their publication, as well as for all his invaluable support in the framework of these analyses. The radiocarbon dating of the samples was financed by the Myrina Kastro project on rock-cut features and rock-art. The publication of the article in OA mode was financially supported by HEAL-Link.

Declaration of interests. The authors declare that they have no known competing financial interests or personal relationships that could have appeared to influence the work reported in this paper.

References

- Acheillara L (2005) *The coroplastic art of Lesbos* [in Greek]. vols. I-II. Ministry of Culture.
- Admiralty 1998. Admiralty Chart, number 1636: *Plans in the Northern Aegean Sea*. Taunton: United Kingdom Hydrographic Office.
- Aerts-Bijma AT, Meijer HAJ, van der Plicht J (1997) AMS sample handling in Groningen. *Nuclear Instruments and Methods B123*, 221–225.
- Anonymous (1993) *Geological map of Greece 1 :50.000. Lemnos island* [in Greek]. Athens: IGME, Institute of Geology & Mineral Exploration.
- Archontidou-Argyri A (2000) Myrina under the light of excavations. Hellenic workshops of Hephaestia and Myrina [in Greek]. In *Lemnos Amichthaloessa*. Athens: Ministry of Culture, 26–34; 42–43.
- Bannister JV (1975) Shell parameters in relation to zonation in Mediterranean limpets. *Marine Biology* **31**, 63–67.
- Beschi L (2001) I disiecta membra di un santuario di Myrina (Lemno). *Annuario della Scuola Archeologica di Atene e delle Missioni Italiane in Oriente LXXIX*, ser. **III**(1), 191–251.
- Bronk Ramsey C (2009) Bayesian analysis of radiocarbon dates. *Radiocarbon* **51**(1), 337–360.
- Bronk Ramsey C and Lee S (2013) Recent and planned developments of the program OxCal. *Radiocarbon* **55**(2), 720–730. doi: [10.1017/S0033822200057878](https://doi.org/10.1017/S0033822200057878)
- Casford JSL, Rohling EJ, Abu-Zied R, Cooke S, Fontainer C, Leng M and Lykousis V (2002) Circulation changes and nutrient concentrations in the late Quaternary Aegean Sea: a nonsteady state concept for sapropel formation. *Paleoceanography* **17**(2), 1024–1034.
- Davies PS (1969) Effect of environment on metabolic activity and morphology of Mediterranean and British species of *Patella*. *Pubblicazioni della Stazione Zoologica di Napoli* **37**, 641–656.
- Facorellis Y, Maniatis Y and Kromer B (1998) Apparent ^{14}C ages of marine mollusk shells from a Greek island—calculation of the marine reservoir effect in the Aegean Sea. *Radiocarbon* **40**(2), 963–974.
- Facorellis Y, Mari A and Oberlin C (2017) The cave of Pan, Marathon, Greece—AMS dating of the Neolithic phase and calculation of the regional marine reservoir effect. *Radiocarbon* **59**(5), 1475–1485.
- Facorellis Y and Vardala-Theodorou E (2015) Sea surface radiocarbon reservoir age changes in the Aegean Sea from about 11,200 BP to present. *Radiocarbon* **57**(3): 491–503.
- Filaniotou O (2012) New data from the recent archaeological excavations in Lemnos. *Annuario della Scuola Archeologica di Atene e delle Missioni Italiane in Oriente LXXXVIII*, ser. **III**(10), 309–346.
- Fornadel AP, Voudouris PC, Spry PG and Melfos V (2012) Mineralogical, stable isotope, and fluid inclusion studies of spatially related porphyry Cu and epithermal Au-Te mineralization, Fakos Peninsula, Limnos Island, Greece. *Mineralogy and Petrology* **105** (1), 85–111.
- Gläser L, Grosche A, Voudouris PC and Haase KM (2022) The high-K calc-alkaline to shoshonitic volcanism of Limnos, Greece: implications for the geodynamic evolution of the northern Aegean. *Contributions to Mineralogy and Petrology* **177**, 73.
- Goslar T, Pazdur MF (1985) Contamination studies on mollusk shell samples. *Radiocarbon* **27**(1), 33–42.
- Heaton TJ, Köhler P, Butzin M, Bard E, Reimer RW, Austin WEN, Bronk Ramsey C, Grootes PM, Hughen KA, Kromer B, Reimer PJ, Adkins J, Burke A, Cook MS, Olsen J, Luke C and Skinner LC (2020) Marine20—the marine radiocarbon age calibration curve (0–55,000 cal BP). *Radiocarbon* **62**(4), 779–820.
- Hedges REM, Law IA, Bronk CR and Housley RA (1989) The Oxford Accelerator Mass Spectrometry Facility: technical developments in routine dating. *Archaeometry* **31**(2), 99–113.

- Hellenic Ministry of Culture (1999) *Καστρών Περιπλοῦς*, 2nd edn. Athens: Hellenic Ministry of Culture, 56–57.
- Marangou C (2006) Land and sea connections: the Kastro rock-cut site (Lemnos island, Aegean Sea, Greece). In Blue L, Hocker F and Englert A (eds), *Connected by the Sea*. Proceedings of the 10th International Symposium on Boat and Ship Archaeology (Roskilde 2003): Oxford: Oxbow Books, 130–136.
- Marangou C (2009) Carved rocks, functional and symbolic (Lemnos island, Greece). In Seglie D, Otte M, Oosterbeek L and Remacle L (eds), *Prehistoric Art: Signs, Symbols, Myth, Ideology*. XVth World Congress of the IUPPS (Lisboa 2006). Oxford: BAR International Series 2028, 93–101.
- Marangou C (2012) A constructed maritime landscape: the carved setting at Myrina Kastro (Island of Lemnos, Greece). In Henderson J (ed), *Beyond Boundaries*. Proceedings of the 3rd International Congress on Underwater Archaeology (London 2008), IKUWA 3. Bonn: Dr. Rudolf Habelt GmbH, 269–276.
- Marangou C (2016) On-going research at Myrina Kastro, Lemnos island: current matters and points at issue. In Spasova D (ed), *Megalithic Monuments and Cult Practices*. Proceedings of the Second International Symposium (Blagoevgrad, October 2016). Blagoevgrad: Neofit Rilski University Press, 185–194.
- Marangou C (2019) Nature as a scenery for symbolic behaviours in the Early Aegean [in Greek]. In *Sanctuaries and Cults in the Aegean from the Early Historic Times to the End of the Late Antiquity, International Congress, Lemnos, 11–15 September 2019*, abstracts volume. Lesbos: Ministry of Culture and Sports, 174–175.
- Marangou C (2020a) Rocks and the sea at Myrina Kastro, Lemnos island. In Davis B and Laffineur R (eds), *Neoteros: Studies in Bronze Age Aegean Art and Archaeology in Honor of Professor John G. Younger on the Occasion of his Retirement* (Vol. 44). Peeters Publishers, 261–270. <https://doi.org/10.2307/j.ctv1q26kwq>
- Marangou C (2020b) Rocky Coast-line, Natural Place and Human Landscape: Myrina Kastro (Lemnos Island, North-East Aegean Sea). In Spasova D and Genov A (eds), *Megalithic Monuments and Cult Practices*. Blagoevgrad: Neofit Rilski University Press, 57–71.
- Marangou C (2021) A rock-cut landscape by the sea: Myrina Kastro in prehistory and antiquity (Lemnos island, North Aegean Sea, Greece). In Sciuto C, Lamesa A, Whitaker K and Yamaç A (eds), *Carved in Stone. The Archaeology of Rock-Cut Sites and Stone Quarries*. Oxford: BAR International Series 3054, 67–76.
- Marangou C, Veropoulidou V and Yannouli E (2014) A “Significant Place” at the Rock-Cut Site of Myrina Kastro, Lemnos Island, in Vasif Sahoglu, Mustafa V. Koc, Elizabeth Greene, Justin Leidwanger (organizers), session T01S022. *A Matrix of Socioeconomic Connectivity: Ports, Harbors and Anchorages in the Mediterranean*. EAA 20th Meeting, Istanbul 10–14 September 2014, abstracts volume, 78.
- Mercone D, Thomson J, Croudace IW, Siani G, Paterne M and Troelstra S (2000) Duration of S1, the most recent sapropel in the eastern Mediterranean Sea, as indicated by accelerator mass spectrometry radiocarbon and geochemical evidence. *Paleoceanography* **15**(3), 336–347.
- Panagopoulos G, Panagiotaras D and Giannouloupoulos P (2013) Groundwater quality assessment of the Limnos Island volcanic aquifers, Greece. *Water Environment Research* **85**(5), 422–433.
- Pavlopoulos K, Fouache E, Sidiropoulou M, Triantaphyllou M, Vouvalidis K, Syrides G, Gonnet A and Greco E (2013) Palaeoenvironmental evolution and sea-level changes in the coastal area of NE Lemnos Island (Greece) during the Holocene. *Quaternary International* **308–309**, 80–88.
- Pe-Piper G, Piper DJW, Koukouvelas I, Dolansky LM and Kokkalas S (2009) Postorogenic shoshonitic rocks and their origin by melting underplated basalts: the Miocene of Limnos, Greece. *Geological Society of America Bulletin* **121**, 39–54.
- Reimer P, Austin W, Bard E, Bayliss A, Blackwell P, Bronk Ramsey C, Butzin M, Cheng H, Edwards RL, Friedrich M, Grootes PM, Guilderson TP, Hajdas I, Heaton TJ, Hogg AG, Hughen KA, Kromer B, Manning SW, Muscheler R, Palmer JG, Pearson C, van der Plicht J, Reimer RW, Richards DA, Scott EM, Southon JR, Turney CSM, Wacker L, Adolphi F, Büntgen U, Capano M, Fahrni SM, Fogtmann-Schulz A, Friedrich R, Köhler P, Kudsk S, Miyake F, Olsen J, Reinig F, Sakamoto M, Sookdeo A and Talamo S (2020) The IntCal20 Northern Hemisphere radiocarbon age calibration curve (0–55 cal kBP). *Radiocarbon* **62**(4), 725–757.
- Rougou K (2013) *The Cult of Cybele in the North-East Aegean: Lesbos, Chios, Lemnos* [in Greek]. PhD dissertation, University of Ioannina, School of Philosophy, Section of History and Archaeology.
- Seila G, Robotti CA and Biglione V (1993) Genetic divergence among three sympatric species of Mediterranean Patella (Archaeogastropoda). *Marine Biology* **115**, 401–405.
- Siani G, Paterne M, Arnold M, Bard E, Métyvier B, Tisnerat N and Bassinot F (2000) Radiocarbon reservoir ages in the Mediterranean Sea and Black Sea. *Radiocarbon* **42**(2), 271–280.
- Siani G, Paterne M, Michel E, Sulpizio R, Sbrana A, Arnold M and Haddad G (2001) Mediterranean Sea surface radiocarbon reservoir age changes since the Last Glacial Maximum. *Science* **294**(5548), 1917–1920; supplemental online files at <http://www.sciencemag.org/cgi/content/full/294/5548/1917/DC1>
- Stuiver M and Braziunas TF (1993) Modeling atmospheric ¹⁴C influences and ¹⁴C ages of marine samples to 10,000 BC. *Radiocarbon* **35**(1), 137–189.
- Stuiver M, Pearson GW and Braziunas T (1986) Radiocarbon age calibration of marine samples back to 9,000 cal yr BP. *Radiocarbon* **28**(2B), 980–1021.
- Stuiver M, Reimer PJ and Braziunas TF (1998) High-precision radiocarbon age calibration for terrestrial and marine samples. *Radiocarbon* **40**(3), 1127–1151.

- Sveinbjörnsdóttir ÁE, Heinemeier J, Arneborg J, Lynnerup N, Ólafsson G and Zoëga G (2010) Dietary reconstruction and reservoir correction of ^{14}C dates on bones from pagan and early Christian graves in Iceland. *Radiocarbon* **52**(2–3), 682–696.
- van der Plicht J, Wijma S, Aerts AT, Pertuisot MH and Meijer HAJ (2000) Status report: the Groningen AMS facility. *Nuclear Instruments and Methods* **B172**, 58–65.
- Wijma S and van der Plicht J (1997) The Groningen AMS Tandatron. *Nuclear Instruments and Methods* **B123**, 87–92.

Cite this article: Facorellis Y, Marangou C, Ntinou M, and Veropoulidou R. Radiocarbon dating of samples connected to rock-cut features at Myrina Kastro (Lemnos Island, Greece) and calculation of the regional marine reservoir effect in the Late Bronze Age in the Aegean Sea. *Radiocarbon*. <https://doi.org/10.1017/RDC.2024.69>